Electronic structure and chemical bonding between the first row transition metals and C_2: A photoelectron spectroscopy study of MC_2^- (M=Sc, V, Cr, Mn, Fe, and Co)

Xi Li and Lai-Sheng Wang[a)]
Department of Physics, Washington State University, Richland, Washington 99352
and W. R. Wiley Environmental Molecular Sciences Laboratory, Pacific Northwest National Laboratory, Richland, Washington 99352

(Received 2 June 1999; accepted 16 August 1999)

Vibrationally resolved photoelectron spectra of MC_2^- (M=Sc, V, Cr, Mn, Fe, and Co) are reported at two detachment photon energies, 532 and 355 nm. All the spectra showed a well resolved vibrational progression in the ground state detachment features. Electron affinities, vibrational frequencies, and information about the low-lying electronic states were obtained for the first row transition metal dicarbide molecules. The measured electron affinities for the MC_2 species show strong metal-dependence with a minimum at VC_2 and a maximum at MnC_2. The ground state vibrational frequencies were observed to decrease from ScC_2 to a minimum in CrC_2 and then increases slightly in MnC_2 and FeC_2. The trends of the electron affinities and vibrational frequencies for the MC_2 species were found to correlate well with the corresponding monoxides, suggesting that the chemical bonding in $M-C_2$ is analogous to that in M–O. The $M-C_2$ bonding was thus interpreted to be quite ionic, and MC_2 can be qualitatively viewed as $M^{2+}C_2^{2-}$, analogous to $M^{2+}O^{2-}$. © *1999 American Institute of Physics.* [S0021-9606(99)00742-4]

I. INTRODUCTION

Carbon forms a range of interesting nanoclusters with transition metals. The rare earth elements can form endohedral fullerenes whereas no other transition metals have been found to do so.[1,2] On the other hand, early transition metals have been found to form stable gas phase metal–carbon cluster ions, known as metallocarbohedrenes (met–cars), with a $M_8C_{12}^+$ stoichiometry.[3–5] Finally, late transition metals are known to be catalysts for carbon nanotube formation.[6,7] The nature of the chemical bonding between carbon and the different metals dictates what type of structures is formed. Small metal–carbon clusters provide an ideal medium to obtain a detailed understanding of the metal–carbon interactions, which is important to gain insight into the growth mechanisms of the various metal–carbon nanomaterials. While significant experimental and theoretical efforts have been directed at small rare earth metal–carbon clusters to understand the formation mechanisms of endohedral fullerenes,[8–16] there have been no systematic investigations of metal–carbon clusters across the Periodic Table, other than the extensive work on met–cars.[17,18] Systematic understanding of the periodic trend of small metal carbon clusters across the first row transition metals will be critical to understand why the different nanostructures are formed.

Our interest has been to probe the electronic structure and bonding of metal–carbon clusters using anion photoelectron spectroscopy (PES). We have investigated the electronic structure of met–cars and a series of titanium–carbon clusters.[19–23] In the present work, we report a systematic investigation of the MC_2 clusters across the first transition series from Sc to Co. Because of the importance of C_2 in the gas phase, the MC_2 clusters may be considered to be the most important metal–carbon clusters; C_2 plays an essential role in the structure of met–cars and MC_2 has been proposed to be the building block in the formation of met–cars. Surprisingly, very little is known about these basic metal–carbon clusters. Theoretically, only ScC_2, TiC_2, and FeC_2 have been investigated.[24–29] We previously reported a PES study of FeC_2^- at a lower instrumental resolution.[30] We recently investigated a series of TiC_x clusters, including TiC_2.[23]

Here we present vibrationally resolved PES spectra for MC_2^- involving the first row transition metals (M=Sc, V, Cr, Mn, Fe, and Co). Electron affinities (EAs), vibrational frequencies, and information about the low-lying electronic energy levels are reported for the neutral MC_2 clusters.

II. EXPERIMENT

The experiments were carried out using a magnetic-bottle PES apparatus with a laser vaporization cluster source. Details of the experiments have been published elsewhere;[31,32] only a brief description is given here. The MC_2^- anions were produced by laser vaporization of the respective metal targets with a helium carrier-gas containing 5% CH_4. Metal–carbon mixed clusters were formed through plasma reactions between laser-ablated metal atoms and CH_4. Cluster species, entrained in the helium carrier-gas, underwent a supersonic expansion and formed a collimated beam with a 6 mm diam skimmer. The anions were extracted perpendicularly from the beam into a time-of-flight (TOF) mass spectrometer. The anions of interest were mass-selected

a)Author to whom correspondence should be addressed. Electronic mail: LS.WANG@PNL.GOV

TABLE I. Observed adiabatic (ADE) and vertical (VDE) binding energies, vibrational frequencies, and low-lying electronic states for ScC_2, VC_2, CrC_2, MnC_2, FeC_2, and CoC_2.

		ADE (eV)[a]	VDE (eV)	ΔE (eV)[b,c]	Vib. freq. (cm^{-1})[c]
ScC_2	*X*	1.65(0.03)	1.73(0.03)	0	670(40)
	A	1.94(0.03)	2.01(0.03)	0.29(0.03)	550(60)
	B	2.75(0.05)		1.10(0.03)	
VC_2	*X*	1.42(0.02)	1.56(0.2)	0	550(40)
	A	1.90(0.02)	1.96(0.02)	0.48(0.02)	520(50)
	B	2.91(0.02)	2.97(0.02)	1.49(0.02)	480(40)
	C	3.13(0.03)		1.71(0.02)	370(40)
CrC_2	*X*	1.63(0.01)	1.70(0.01)	0	510(30)
	A	2.02(0.01)	2.09(0.01)	0.39(0.01)	540(30)
	B	2.33(0.03)		0.70(0.02)	
	C	2.47(0.03)		0.84(0.02)	480(60)
	D	2.68(0.03)		1.05(0.02)	
	E	2.88(0.03)		1.25(0.02)	540(60)
	F	3.01(0.03)	3.08(0.03)	1.38(0.02)	550(60)
	G	3.40(0.03)		1.77(0.02)	
MnC_2	*X*	2.12(0.01)	2.25(0.01)	0	520(30)
	A	2.86(0.02)		0.74(0.01)	450(40)
	B	3.06(0.02)		0.94(0.02)	330(40)
FeC_2	*X*	1.98(0.01)	2.12(0.01)	0	560(30)
	A	2.98(0.03)	3.04(0.03)	1.00(0.02)	480(50)
	B	3.16(0.03)	3.22(0.03)	1.18(0.02)	420(60)
CoC_2	*X*	1.70(0.07)		0	540(60)
	A	2.62(0.05)		0.92(0.06)	

[a]The ADE of the ground state feature (*X*) represents the adiabatic electron affinity.
[b]The excitation energies relative to the ground state (*X*).
[c]Relative energies were measured more accurately.

and decelerated before crossing with a detachment laser beam. Two photon energies (532 nm–2.331 eV and 355 nm–3.496 eV) from a Q-switched Nd:YAG laser were used for the current investigation. The photoemitted electrons were collected by the magnetic-bottle at nearly 100% efficiency and analyzed in a 3.5 m long TOF tube. Photoelectron TOF spectra were collected at a 10 Hz repetition rate and were converted to electron binding energies calibrated by the known spectrum of Cu^-. VC_2^- and CrC_2^- were also produced by laser vaporization of the respective solid carbide targets with a pure helium carrier-gas. The same PES spectra were obtained as using pure metal targets and a CH_4-containing He carrier-gas. The resolution of the magnetic-bottle electron analyzer was about $\Delta E/E \sim 2\%$, i.e., $\sim$20 meV for one eV electrons. The further improvement of our magnetic-bottle apparatus can be found in a recent publication.[33]

III. RESULTS

The PES spectra are shown in Figs. 1–6 at the two photon energies (532 and 355 nm) for MC_2^-, M=Sc, V, Cr, Mn, Fe, and Co, respectively. The observed detachment transitions are labeled with the alphabets and the vertical lines represent resolved vibrational structures. The observed binding energies and vibrational frequencies are summarized in Table I for all the six MC_2 species investigated currently.

A. ScC_2^-

The spectra of ScC_2^- are shown in Fig. 1. The 532 nm spectrum exhibits two bands partially overlapping. The ground state band (*X*) shows a well-resolved vibrational progression with a spacing of 670 (40) cm^{-1}. The 0–0 transition of the *X* band at 1.65 eV defines the adiabatic electron affinity (EA) of ScC_2. Two hot band features (HB) were clearly observed which have a smaller spacing of $\sim$500 (80) cm^{-1}. The *A* band was less well-resolved due to the overlap with the ground state features. A vibrational spacing of 550 (60) cm^{-1} was estimated. A weak and broad feature (*X′*) was also observed at the lower binding energy (BE) side. The intensity of this feature could be enhanced under certain source conditions, but could not be completely eliminated. It was either due to an isomer or due to an electronically excited state of ScC_2^-. The 355 nm spectrum revealed almost continuous, weak signals through the entire high BE side, probably due to closely spaced low-lying electronic states of ScC_2. We were only able to definitely identify a feature *B* at $\sim$2.75 eV. The intensity of the *A* band was observed to be significantly reduced in the 355 nm spectrum.

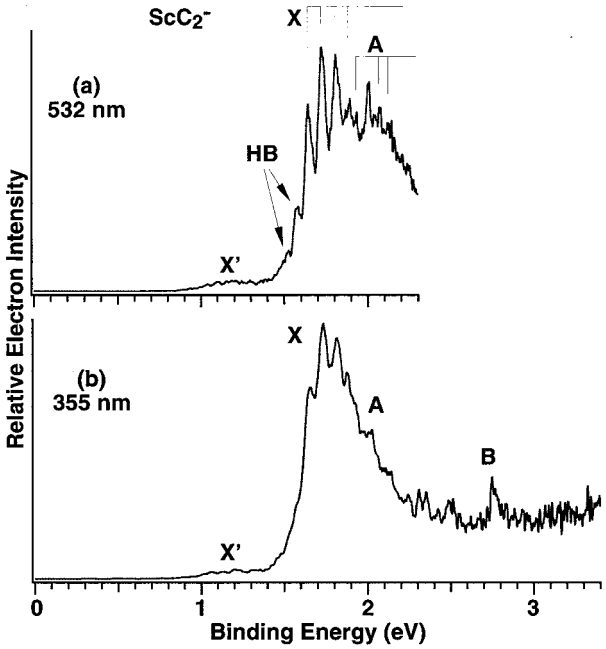

FIG. 1. Photoelectron spectra of ScC_2^- at (a) 532 nm and (b) 355 nm. HB stands for hot band transitions.

B. VC_2^-

The spectra of VC_2^- are shown in Fig. 2. The 532 nm spectrum revealed an intense and well resolved vibrational progression (*X*) due to the ground state of VC_2 with a spacing of 550 (40) cm^{-1}. The 0–0 transition of the *X* band yielded an EA of 1.42 eV for VC_2. Several weak features were also observed in the 532 nm spectrum and were tentatively identified as a vibrational progression (*A*) with a spacing of $\sim$520 cm^{-1}. At 355 nm, two intense bands (*B* and *C*) near 3 eV BE were clearly observed with well resolved vibrational structures. The *B* band has a vibrational frequency of 480 (40) cm^{-1}, whereas the *C* band has a smaller spacing of 370 (40) cm^{-1}. There also seemed to be weak features between 2.2 and 2.9 eV in the 355 nm spectrum, probably

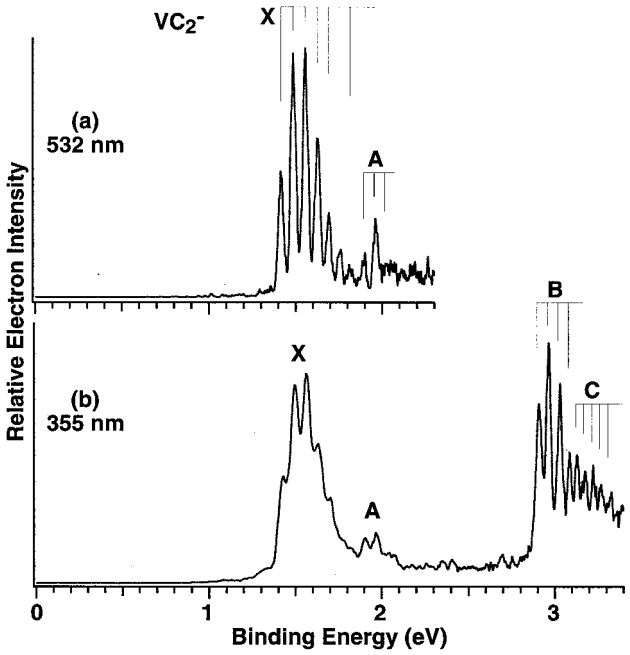

FIG. 2. Photoelectron spectra of VC_2^- at (a) 532 nm and (b) 355 nm.

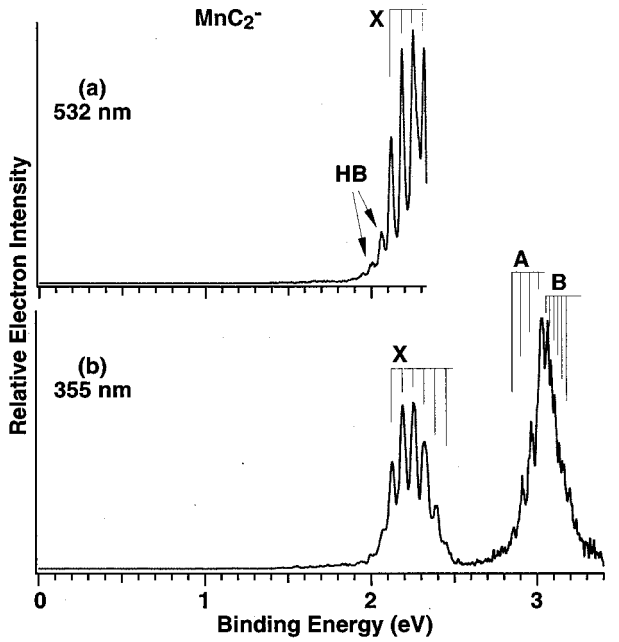

FIG. 4. Photoelectron spectra of MnC_2^- at (a) 532 nm and (b) 355 nm. HB stands for hot band transitions.

due to low-lying excited states of VC_2, but they could not be definitively identified due to their weak intensities.

C. CrC_2^-

The spectra of CrC_2^- are shown in Fig. 3. The 532 nm spectrum showed two well resolved vibrational progressions. The ground state progression (*X*) yielded a vibrational frequency of 510 (30) cm^{-1} and an EA of 1.63 eV for CrC_2. Two hot band features were also visible at the lower BE side with a smaller spacing of ~450 (60) cm^{-1}. The *A* band yielded a vibrational frequency of 540 (30) cm^{-1}. A rising tail at the high BE side of the 532 nm spectrum indicated more electronic states at higher BE. Indeed the 355 nm spectrum of CrC_2^- revealed a complicated and congested spectral pattern, and at least six more electronic transitions were observed beyond the 532 nm photon energy range. These additional states are labeled from *B* to *G* in Fig. 3(b), and vibrational structures were clearly observed for the *C*, *E*, and *F* states as indicated in the figure.

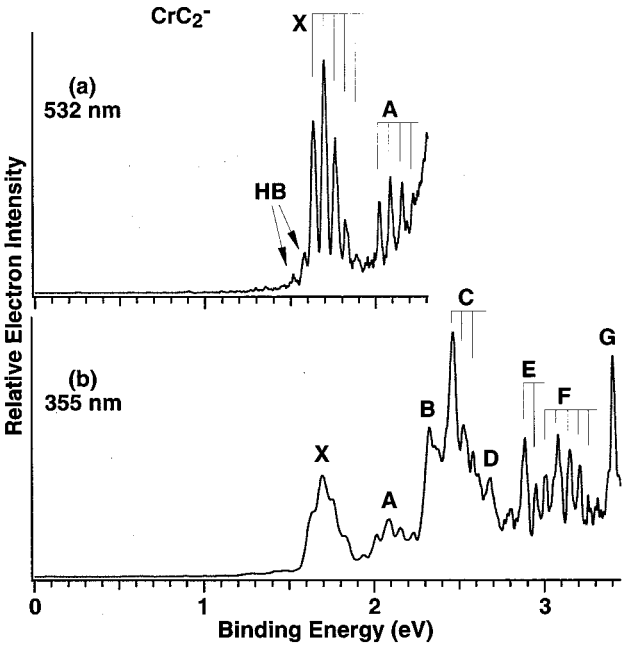

FIG. 3. Photoelectron spectra of CrC_2^- at (a) 532 nm and (b) 355 nm. HB stands for hot band transitions.

D. MnC_2^-

The spectra of MnC_2^- are shown in Fig. 4. The MnC_2^- spectra appeared to have rather high binding energies. At 532 nm, a well resolved vibrational progression was only partially observed, yielding a frequency of 520 (30) cm^{-1} and an EA of 2.12 eV for MnC_2. Weak hot band features were clearly observed at the lower BE side, with a smaller spacing of ~450 (50) cm^{-1}. The 355 nm spectrum only revealed one extra band near 3 eV. Upon closer examination, the higher BE band actually was consisted of two overlapping bands with different vibrational spacings. On the lower BE side, a progression (*A*) with a spacing of 450 (40) cm^{-1} could be clearly identified. The progression on the higher BE side (*B*) was more difficult to identify because of the overlap with the *A* band and its smaller vibrational spacing, which was estimated to be ~330 (40) cm^{-1}.

E. FeC_2^-

The spectra of FeC_2^- appeared to be similar to that of MnC_2^-, as shown in Fig. 5, except that a weak low BE (*X'*) feature was observed in the FeC_2^- spectra and that the two higher BE features (*A* and *B*) were better separated in the 355

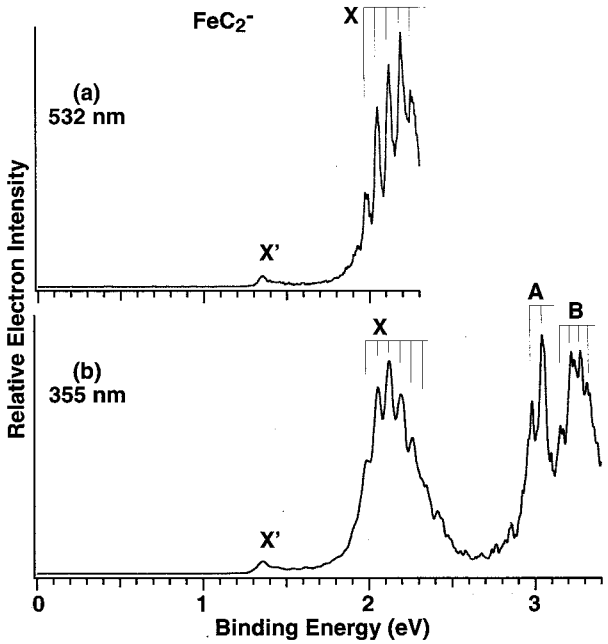

FIG. 5. Photoelectron spectra of FeC_2^- at (a) 532 nm and (b) 355 nm.

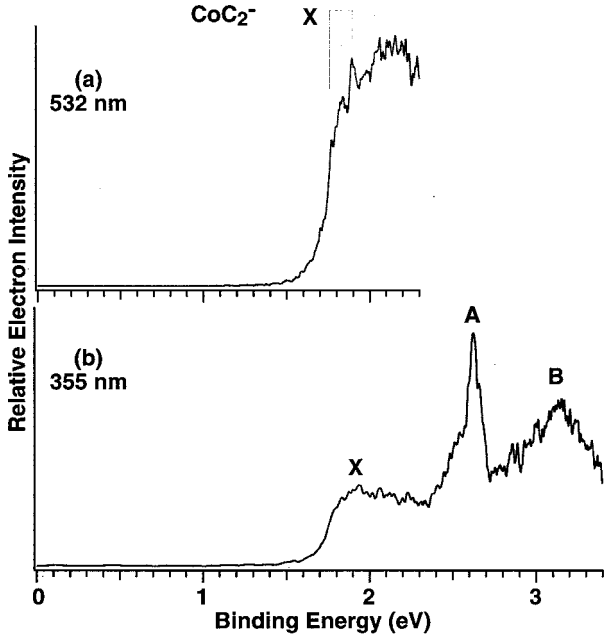

FIG. 6. Photoelectron spectra of CoC_2^- at (a) 532 nm and (b) 355 nm.

nm spectrum of FeC_2^- [Fig. 5(b)]. The 532 nm spectrum showed a well resolved vibrational progression, which was cut off at the high BE side. A vibrational frequency of 560 (30) cm^{-1} was obtained. The EA of FeC_2 was measured to be 1.98 eV from the BE of the 0–0 transition. The weak X' feature with a vertical BE of 1.35 (3) eV depended on the source conditions, but could not be eliminated, similar to that in the ScC_2^- spectra (Fig. 1). It was either due to an excited state or due to an isomer of FeC_2^-. The 355 nm spectrum clearly revealed two higher BE bands, each with vibrational structures.

F. CoC_2^-

The CoC_2^- spectra shown in Fig. 6 were broad and congested, quite different from the well resolved spectra of the other MC_2^- species. The 532 nm spectrum appeared to show discernible vibrational features with a spacing of ~540 cm^{-1}, as shown in Fig. 6(a). At 355 nm, a sharp feature (A) was observed at 2.62 eV, as well as a broad feature B at higher BE. However, there were continuous signals throughout the energy range with very little fine features resolved. The EA of CoC_2 was estimated from the onset of the X feature to be ~1.70 eV with a large error bar, as given in Table I.

IV. DISCUSSION

The PES features represent photodetachment transitions from the ground state of the anions to the ground and excited states of the neutrals. The spectra of the MC_2^- species shown in Figs. 1–6 contained information not only about the ground state, but also about the low-lying excited states of the MC_2 neutrals. The excitation energies of the excited states are given in Table I (ΔE) by subtracting the adiabatic binding energies of the ground state (X) from that of the higher BE features. A high density of low-lying excited states was observed for all the MC_2 species, except for MnC_2 and FeC_2, for which only two excited states were observed within ~1 eV above the ground state. CrC_2 appeared to show the richest low-lying excited states with seven well-resolved excited states observed in the 355 nm spectrum [Fig. 3(b) and Table I]. Detailed assignments of the electronic excited states are not possible at present, except for ScC_2 for which detailed calculations are available.[24,25] Therefore, our discussion will start with ScC_2 using the previous calculations. For the other MC_2 species, we will focus on the ground state properties and discuss the periodic trends of the observed EAs and ground-state vibrational frequencies. In particular, we will compare these trends with those of the corresponding monoxides and obtain insight into the nature of the chemical bonding between M and C_2.

A. ScC_2 and possible isomer

Among the MC_2 species of the $3d$ transition-metals, ScC_2, TiC_2, and FeC_2, have been investigated previously and their ground state structures are well understood.[24–29] They all have the triangle C_{2v} structure with the linear MCC structure higher in energy. ScC_2 may be considered the simplest among the $3d$ MC_2 species and its structure and bonding have been investigated theoretically by two groups previously.[24,25] In particular, Roszak and Balasubramanian (RB) have calculated the low-lying electronic states of ScC_2 and its thermodynamic properties.[24] RB obtained two low-lying excited states for the C_{2v} ScC_2 at 0.234 and 1.277 eV, which are in good agreement with the two excited states that we observed for ScC_2 as shown in Table I. RB also calculated the linear ScCC structure, which was found to be-

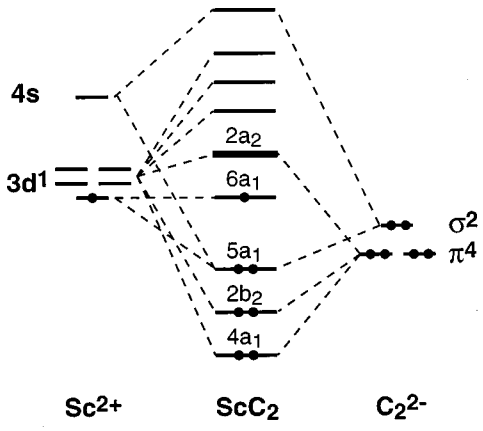

FIG. 7. Schematic diagram showing the molecular orbitals of ScC_2 from Sc^{2+} interacting with C_2^{2-}.

$\sim$0.13 eV higher than the C_{2v} structure when dynamic electron correlation effects were not included. At higher levels of theory, they found that the linear structure was about 0.8 eV higher than the C_{2v} structure and concluded that the ground state of ScC_2 should be the C_{2v} structure unambiguously. The first two low-lying excited states were calculated to be at 0.131 and 0.918 eV for the linear isomer, which were in worse agreement with the experiment than the excitation energies of the C_{2v} structure. However, vibrational frequencies were not calculated, which would have been a valuable parameter to compare with the experimental measurement. Jackson *et al.* have also investigated ScC_2 recently and obtained a C_{2v} ground state structure.[25] Thus, we concluded that the major isomer observed in our experiment should correspond to the C_{2v} species. The weak feature (X', Fig. 1) observed in our experiment was tentatively attributed to the linear isomer. This assignment suggested that the linear isomer should have a lower EA, which needs to be confirmed by theoretical calculations.

The nature of the chemical bonding between Sc and C_2 is quite ionic; RB calculated a 7.49 D dipole moment for ScC_2 with a large electron transfer from Sc to C_2.[24] Thus, ScC_2 can be qualitatively viewed as $Sc^{2+}C_2^{2-}$. In fact, the C–C bond length (1.278 Å) in ScC_2 is quite close to that of a C–C triple bond. Figure 7 shows a qualitative molecular orbital (MO) picture of ScC_2 from Sc^{2+} interacting with C_2^{2-}.[24,25] The π orbitals of C_2^{2-} interact with the $3d$ orbitals of Sc^{2+} and form the $4a_1$ and $2b_2$ bonding MOs. The σ MO of C_2^{2-} interacts with the $4s$ and $3d$ of Sc^{2+} to form the bonding $5a_1$ MO. The $6a_1$ MO is nonbonding, mainly of $3d_{z^2}$ character, which is singly occupied to give a $^2A_1$ ground state for ScC_2. In the ScC_2^- anion, the extra electron can enter either the empty $2a_2$ antibonding MO (thicker bar, Fig. 7) or the singly occupied nonbonding $6a_1$ MO. As discussed next, our observation is consistent with the former. Removal of the $2a_2$ electron from ScC_2^- resulted in the X ground state feature in the PES spectra of ScC_2^- (Fig. 1). The vibrational progression of the X band should be due to the ν_1 Sc–C symmetric stretching mode and suggested that there were significant Sc–C bond length changes between the anion and neutral ground state. The observed hot band transitions gave a smaller vibrational frequency ($\sim$500 cm^{-1}) for the ScC_2^- anion compared to that for the ScC_2 neutral ground state, suggesting that the $2a_2$ MO is indeed antibonding in nature. Detachment of the $6a_1$ electron led to the A feature of the PES spectra. The 550 cm^{-1} vibrational frequency for the A state was similar to that of the ScC_2^- ground state, indicating the nonbonding nature of the $6a_1$ MO.

The nearly continuous signals at the higher BE side of the 355 nm spectrum indicated a high density of low-lying excited states for ScC_2. Many of these states could be due to multielectron transitions in the photodetachment, i.e., removal of one electron and excitation of another electron to a higher MO. Such multielectron transitions, owing to strong electron correlation effects, were previously observed in photoelectron spectra of ScO^-,[34] and other transition metal oxides.[35]

B. Ground state structures of the MC_2 clusters

We have previously studied a series of TiC_x^- clusters, including TiC_2^-,[23] which was proposed to have a C_{2v} structure.[26] Sumathi and Hendickx have carried out a detailed calculation on TiC_2 and confirmed the C_{2v} structure for TiC_2.[27] the bonding in TiC_2 may be considered to be similar to that in ScC_2 and a triplet ground state was obtained for TiC_2. The latter is consistent with the ground state of ScC_2^-, which is isoelectronic with the TiC_2 neutral.

There is no calculation available for the other MC_2 species considered here except for FeC_2. We studied FeC_2^- previously at somewhat lower resolution.[30] The results were considered qualitatively using a linear $FeCC^-$ structure, in analogy to acetylene. However, two subsequent theoretical calculations concluded that the ground state of FeC_2 has a C_{2v} structure.[28,29] The linear FeCC isomer was found to be higher in energy. Our new spectra of FeC_2^- shown in Fig. 5 had much higher quality with well resolved vibrational frequencies and allowed better determination of the EA and excited states of FeC_2, as given in Table I. Our previous consideration of a linear FeC_2 was based on a simple model involving bonding between Fe-$4s$ and C_2. However, if interaction of Fe-$3d$ with C_2 is significant, the C_{2v} structure would be favored. Based on the available theoretical calculations, we suggested that the observed spectral features were most likely due to the C_{2v} species, although conclusive assignments would require calculations on the anions as well. The weak, lower BE feature (X', Fig. 5) was then tentatively attributed to a possible linear isomer, $FeCC^-$. This suggests that the linear isomer would have a smaller EA than the C_{2v} species, similar to the case of ScC_2 mentioned above (Fig. 1). However, we could not rule out the possibility that it was due an electronic excited state of the C_{2v} species. A definitive assignment would require accurate theoretical calculations on both the neutral and anion species.

The structures of the remaining MC_2 species of the $3d$ series are completely unknown. The current data do not provide structural information without theoretical calculations. Further systematic theoretical studies of these MC_2 species would be interesting.

TABLE II. The adiabatic electron affinities (EA, eV) and M–C stretching frequencies (ν, cm^{-1}) of the MC_2 clusters compared to that of the corresponding monoxides.

	Sc	Ti	V	Cr	Mn	Fe	Co
EA (MC_2)[a]	1.65(3)	1.54(3)[b]	1.42(2)	1.63(1)	2.12(1)	1.98(1)	1.70(7)
EA (M–O)	1.35(2)[c]	1.30(3)[d]	1.229(8)[e]	1.221(6)[f]	1.41(2)[g]	1.50(3)[h]	1.45(1)[g]
ν (MC_2)[a]	670(40)	560(50)[b]	550(40)	510(30)	520(30)	560(30)	540(60)
ν (M–O)[i]	1000 (50)[c]	1000.02	1001.8	884.976	832.41	871.52	851.7

[a]Present work.
[b]Reference 23.
[c]Reference 34.
[d]Reference 35.
[e]Reference 37.
[f]Reference 38.
[g]Reference 40.
[h]Reference 39.
[i]Reference 36.

C. Nature of chemical bonding between M and C_2: Periodic trend of EAs and vibrational frequencies and comparison to that of the metal monoxides

The ground state PES band for all the MC_2^- spectra consisted of a vibrational progression, suggesting that there were significant geometry changes between the ground states of the anions and neutrals. In several cases (Figs. 1, 3, and 4), hot band transitions were well resolved. In all these cases, the vibrational frequencies obtained for the anions were smaller than that of the neutrals. The resolved vibrational progression should be due to the M–C symmetric stretching. Therefore, our data suggesting that the extra electron in all the MC_2^- anions occupied an antibonding MO between the metal and C, as discussed above for ScC_2^-,

As seen from Table II and Fig. 8, the ground-state vibrational frequency of ScC_2 is the highest among the $3d$ MC_2 species, and then drops sharply from ScC_2 to TiC_2. CrC_2 has the lowest M–C stretching frequency, which increases slightly in MnC_2 and FeC_2. Interestingly, we found a correlation between the M–C stretching frequencies in MC_2 and the vibrational frequencies of the monoxides,[36] that are also plotted in Fig. 8. The only difference is that there is no sharp drop from ScO to TiO. In fact, the vibrational frequencies of ScO, TiO, and VO are nearly identical with a major drop occurring in CrO and a minimum in MnO.

We also found a correlation between the EAs of MC_2 and those of M–O,[34,35,37–40] as shown in Table II and in Fig. 9. The EAs of MnO and CoO are from our unpublished results.[40] The EAs of the MC_2 species show an interesting trend with a minimum at VC_2 and a maximum at MnC_2. Although the EAs of the oxides do not show as dramatic a change as that of the MC_2 species, the trend of the oxides is very similar to that of MC_2. The higher EAs of the MC_2 species compared to the corresponding M–O diatomics reflect the higher EA of C_2 compared to that of the O atom.

The similar trends in the ground state vibrational frequencies and EAs between the MC_2 and M–O species suggest their similarity in chemical bonding. The O atom is divalent and the M–O bonding is characterized with strong ionic characters. The monoxides can be qualitatively viewed as $M^{2+}O^{2-}$, all with a large dipole moment.[36] On the other hand, C_2 has a very high EA and can be viewed as divalent similar to the O atom. In fact, the C–C bond length in MC_2 is very close to the C–C triple bond for the three MC_2 (M =Sc, Ti, and Fe) that have been studied theoretically.[24–29] Therefore, the chemical bonding between the $3d$ transition metals and C_2 is also characterized with strong ionic bonding characters, and MC_2 may be viewed as $M^{2+}C_2^{2-}$, as discussed above for ScC_2. Hence, we observed a remarkable similarity between the chemical bonding of MC_2 and M–O.

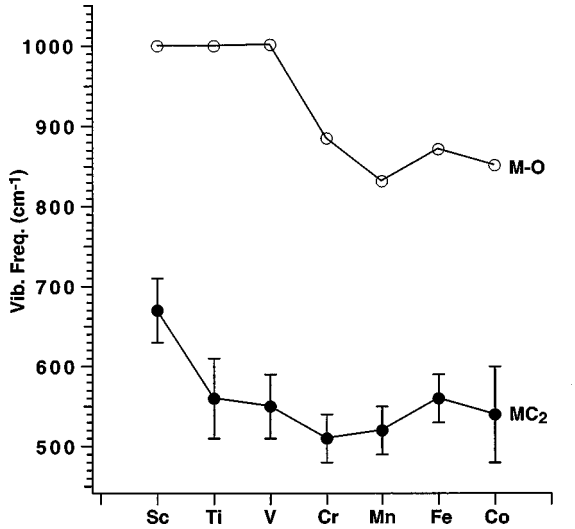

FIG. 8. Ground state vibrational frequencies of the first row transition metal monoxide (M–O) and dicarbides (MC_2).

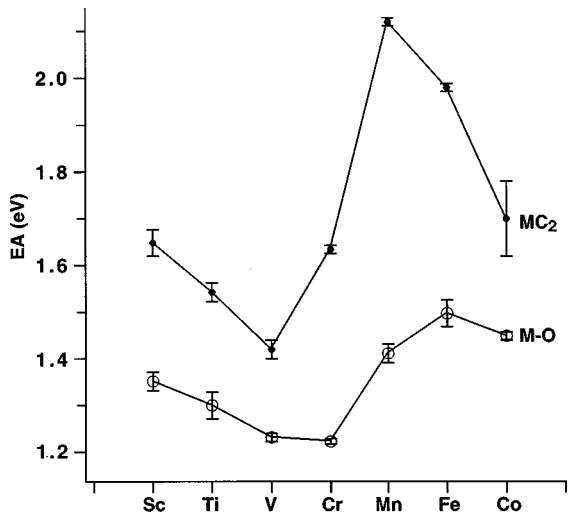

FIG. 9. Electron affinities (EA) of the first row transition metal monoxide (M–O) and dicarbides (MC_2).

However, it is surprising to observe that the Sc–C_2 interactions seemed to be much stronger than that in Ti–C_2 and V–C_2, as seen from the sharp decrease of the M–C stretching frequencies from ScC_2 to TiC_2 in Fig. 8. On the other hand, the bonding strength in the corresponding monoxides is very similar as seen from their nearly identical vibrational frequencies (Fig. 8). One possible interpretation may be proposed based on the MO diagram shown in Fig. 7. Assuming the empty MOs due to the $3d$ orbitals are all antibonding as reflected in the weaker bonding in the ScC_2^- anion, then successive filling of these antibonding MOs in TiC_2 and VC_2 would result in a significant weakening of the M–C_2 bonding. This would suggest that the $3d$-π interactions in MC_2 are much stronger whereas the $3d$-derived MOs in the monoxides are relatively nonbonding. The latter was supported by the fact that the ground state detachment features in all the monoxide photoelectron spectra yielded much shorter vibrational progressions in the ground state,[34,35,37–40] i.e., the extra electron occupies a more nonbonding MO in the monoxide anions. In any case, it appeared that the difference in chemical bonding with carbon between Sc and Ti is already reflected in the MC_2 species. Quantitative understanding of this subtle difference in MC_2 may provide insight into the question why Sc does not form met–car, but forms endohedral fullerenes, whereas Ti and V form met–cars, but do not form endohedral fullerenes.

V. CONCLUSIONS

We reported a systematic study of the electronic structures and chemical bonding between the $3d$ transition metals and C_2. Vibrationally resolved photoelectron spectra of the MC_2^- species (M=Sc, V, Cr, Mn, Fe, and Co) were presented. Electron affinities, vibrational frequencies, and information about the low-lying electronic energy levels were obtained for the MC_2 clusters. The ground state M–C stretching frequencies and the electron affinities for the MC_2 species were found to show similar trend to the corresponding monoxides. Thus experimental evidence was obtained for the similarity between the chemical bonding of MC_2 and M–O, and MC_2 may be viewed as $M^{2+}C_2^{2-}$ in analogy to $M^{2+}O^{2-}$. The significant vibrational progression observed in the ground state detachment transitions in all the MC_2^- species suggested that the extra electron in the MC_2^- anions occupied an antibonding MO. The current experiments provided systematic vibrational and electronic structure information about the $3d$ MC_2 species and will be valuable to compare to systematic theoretical investigations to elucidate the evolution of the chemical bonding between carbon and the transition metals across the first transition series.

ACKNOWLEDGMENTS

Support of this research by the National Science Foundation (DMR-9622733) is gratefully acknowledged. This work was performed at the W. R. Wiley Environmental Molecular Sciences Laboratory, a national scientific user facility sponsored by DOE's Office of Biological and Environmental Research and located at Pacific Northwest National Laboratory, operated for DOE by Battelle. L.S.W. is an Alfred P. Sloan Foundation Research Fellow.

[1] Y. Chai, T. Guo, C. Jin, R. E. Haufler, L. P. F. Chibante, J. Fure, L. Wang, J. M. Alford, and R. E. Smalley, J. Phys. Chem. **95**, 7564 (1991).
[2] D. S. Bethune, R. D. Johnson, J. R. Salem, M. S. de Vries, and C. S. Yannoni, Nature **366**, 123 (1993).
[3] B. C. Guo, K. P. Kerns, and A. W. Castleman, Science **255**, 1411 (1992).
[4] B. C. Guo, S. Wei, J. Purnell, S. Buzza, and A. W. Castleman, Science **256**, 511 (1992).
[5] J. S. Pilgrim and M. A. Duncan, J. Am. Chem. Soc. **115**, 6958 (1993).
[6] S. Iijima and T. Ichihashi, Nature **363**, 603 (1993).
[7] D. S. Bethune, C. H. Kiang, M. S. de Vries, G. Gorman, R. Savoy, J. Vaquez, and R. Beyers, Nature **363**, 605 (1993).
[8] D. E. Clemmer, K. B. Shelimov, and M. F. Jarrold, Nature **367**, 718 (1994).
[9] D. E. Clemmer and M. F. Jarrold, J. Am. Chem. Soc. **117**, 8841 (1995).
[10] K. B. Shelimov and M. F. Jarrold, J. Am. Chem. Soc. **118**, 1139 (1996).
[11] D. S. Yang, M. Z. Zgierski, and P. A. Hackett, J. Chem. Phys. **108**, 3591 (1998).
[12] D. L. Strout and M. B. Hall, J. Phys. Chem. **100**, 18 007 (1996).
[13] D. L. Strout and M. B. Hall, J. Phys. Chem. A **102**, 641 (1998).
[14] S. Roszak and K. Balasubramanian, J. Phys. Chem. **100**, 8254 (1996).
[15] S. Roszak and K. Balasubramanian, J. Chem. Phys. **106**, 158 (1997).
[16] S. Roszak and K. Balasubramanian, J. Phys. Chem. A **102**, 6004 (1998).
[17] M. A. Duncan, J. Cluster Sci. **8**, 239 (1997).
[18] M. M. Rohmer and M. Benard, Chem. Rev. (in press).
[19] L. S. Wang, S. Li, and H. Wu, J. Phys. Chem. **100**, 19 211 (1996).
[20] L. S. Wang and H. Cheng, Phys. Rev. Lett. **78**, 2983 (1997).
[21] S. Li, H. Wu, and L. S. Wang, J. Am. Chem. Soc. **119**, 7417 (1997).
[22] L. S. Wang, X. B. Wang, H. Wu, and H. C. Cheng, J. Am. Chem. Soc. **120**, 6556 (1998).
[23] X. B. Wang, C. F. Ding, and L. S. Wang, J. Phys. Chem. A **101**, 7699 (1997).
[24] S. Roszak and K. Balasubramanian, J. Phys. Chem. A **101**, 2666 (1997).
[25] P. Jackson, G. E. Gadd, D. W. Mackey, H. van der Wall, and G. D. Willett, J. Phys. Chem. A **102**, 8941 (1998).
[26] B. V. Reddy and S. N. Khanna, J. Phys. Chem. **98**, 9446 (1994).
[27] R. Sumathi and M. Hendrickx, Chem. Phys. Lett. **287**, 496 (1998).
[28] B. K. Nash, B. K. Rao, and P. Jena, J. Chem. Phys. **105**, 11 020 (1996).
[29] Z. Cao, J. Mol. Struct.: THEOCHEM **365**, 211 (1996).
[30] J. Fan and L. S. Wang, J. Phys. Chem. **98**, 11 814 (1994).
[31] L. S. Wang, H. S. Cheng, and J. Fan, J. Chem. Phys. **102**, 9480 (1995).
[32] L. S. Wang and H. Wu, in *Advances in Metal and Semiconductor Clusters. IV. Cluster Materials*, edited by M. A. Duncan (JAI, Greenwich, 1998), p. 299.
[33] L. S. Wang, C. F. Ding, X. B. Wang, and S. E. Barlow, Rev. Sci. Instrum. **70**, 1957 (1999).
[34] H. Wu and L. S. Wang, J. Phys. Chem. A **102**, 9129 (1998).
[35] H. Wu and L. S. Wang, J. Chem. Phys. **107**, 8221 (1997).
[36] A. J. Merer, Annu. Rev. Phys. Chem. **40**, 407 (1989).
[37] H. Wu and L. S. Wang, J. Chem. Phys. **108**, 5310 (1998).
[38] P. G. Wenthold, R. F. Gunion, and W. C. Lineberger, Chem. Phys. Lett. **258**, 101 (1996).
[39] J. Fan and L. S. Wang, J. Chem. Phys. **102**, 8714 (1995).
[40] X. Li and L. S. Wang (unpublished).